

# Local structure and defect chemistry of substituted lithium manganese spinels: X-ray absorption and computer simulation studies

Brett Amundsen<sup>a,b,\*</sup>, M. Saiful Islam<sup>c</sup>, Deborah J. Jones<sup>a</sup>, Jacques Rozière<sup>a</sup>

<sup>a</sup> *Laboratoire des Agrégats Moléculaires et Matériaux Inorganiques ESA CNRS 5072, Université Montpellier 2, Place Eugène Bataillon, 34095 Montpellier Cédex 5, France*

<sup>b</sup> *School of Chemical and Physical Sciences, Victoria University of Wellington, P.O. Box 600, Wellington, New Zealand*

<sup>c</sup> *Department of Chemistry, University of Surrey, Guildford, Surrey GU2 5XH, UK*

## Abstract

The charge distributions and effects on local structure resulting from substitution of Mn by Ti, Cr, Co and Ga in  $\text{LiMn}_2\text{O}_4$  are determined by X-ray absorption spectroscopy. Atomistic simulation methods are used to obtain additional insights into local structure and to calculate the energetics of lithium disorder and migration in lattices containing these substitutional ions or Li on octahedral Mn sites. The formation of protonic species in spinel lithium manganates is discussed in relation to a tetrahedral–octahedral vacancy pair model. © 1999 Elsevier Science S.A. All rights reserved.

**Keywords:** Spinel; Lithium manganese oxides; Cation substitution; X-ray absorption fine structure spectroscopy; Computer simulation

## 1. Introduction

The use of lithium manganese spinels in advanced batteries depends on their properties vis-à-vis the extraction and insertion of lithium ions. These compounds are particularly versatile in terms of tailoring their electrochemical properties, as they are able to incorporate large amounts of substitutional ions and changes in lithium and oxygen stoichiometry while retaining the spinel crystal structure. Many studies have examined the effects of changes in composition on bulk structure and properties. However, local structural and electronic perturbations introduced by defect species can affect the behaviour of lithium ions in the lattice and will therefore determine key electrochemical properties such as the electrode capacity and rate capability. Knowledge of the local modifications associated with lattice defects should lead to new insights into the chemistry and electrochemistry of lithium manganese spinels, and to the design and development of materials having desired chemical and electronic properties.

Partial substitution of Mn in  $\text{LiMn}_2\text{O}_4$  has been extensively investigated for its effects on electrochemical prop-

erties [1,2]. In particular, the problem of capacity fading in  $\text{LiMn}_2\text{O}_4$  electrodes, which is believed to be at least partly due to the formation of domains of tetragonally-distorted  $\text{Mn}^{3+}$ -rich phase at high levels of reduction, has been successfully addressed by substitution to decrease the  $\text{Mn}^{3+}/\text{Mn}^{4+}$  ratio [3,4]. However, the choice of substitutional ion and its oxidation state may modify the electrode in other ways, depending on the chemical characteristics of the ion. The objectives of the work presented here are to characterise the charge distributions and local structures associated with a range of substitutional ions in  $\text{LiMn}_2\text{O}_4$ , and to determine the effects of the substitutions on lithium site energies, lithium migration and defect formation.

## 2. Experimental

$\text{LiA}_x\text{Mn}_{2-x}\text{O}_4$  compounds with A = Cr, Co, Ga or Ti were prepared by heating intimately ground mixtures of the corresponding salts or oxides in three cycles under air to temperatures between 600 and 750°C. All the compounds described were single-phase spinels as characterised by powder X-ray diffraction. Compositions were determined by flame spectrometry and chemical titrations. Our methods of sample preparation and data analysis for X-ray absorption experiments have been described previously [5].

\* Corresponding author. Tel.: +33-4-67-14-33-40; Fax: +33-4-67-14-33-04; E-mail: debtoja@univ-montp2.fr

Atomistic simulations were performed using lattice energy minimisation techniques embodied in the code GULP [6]. The basis of the simulations is a Born potential model for the  $\text{LiA}_x\text{Mn}_{2-x}\text{O}_4$  compound which describes the energy of the lattice as a function of the atomic coordinates. Interatomic interactions within the lattice are described by two-body potentials which include both long-range Coulombic interactions and short-range terms due to electronic repulsions and Van der Waals forces. Ionic polarisability is incorporated by the shell model [7], which allows the dielectric response to point defects to be modeled. The potential and shell model parameters are derived from simulations of the binary oxides and are described in earlier work [8,9]. The Mott–Littleton approach [10] is used to model defects in the lattices. Ionic relaxations in a spherical region containing ca. 200 atoms surrounding the defect are calculated explicitly, while interactions between the defect and more distant regions of the crystal are determined by quasi-continuum methods using the dielectric properties of the compound.

### 3. Results and discussion

#### 3.1. Charge distribution and local order in substituted lithium manganates

X-ray absorption allows the local environments of the substitutional element and the manganese ions to be probed independently in the same compound. X-ray absorption spectroscopy therefore provides information both about the electronic state and structural environment of the substitutional ion, and about the effect of the substitution on the electronic state and structural environment of the manganese. The series of spectra which we have recorded at the Ti, Cr and Co *K*-edges are consistent with the oxidation states  $\text{Ti}^{4+}$ ,  $\text{Cr}^{3+}$  and  $\text{Co}^{3+}$  in  $\text{LiA}_x\text{Mn}_{2-x}\text{O}_4$  compounds, and contain near-edge (XANES) resonances identical to those observed for Mn in  $\text{LiMn}_2\text{O}_4$ . This near-edge structure has been analysed using multiple scattering theory and shown to be characteristic of the octahedral site in spinel lithium manganates [11].

Quantitative structural information including coordination numbers and interatomic distances can be obtained by analysing the extended X-ray absorption fine structure (EXAFS) which extends up to 1000 eV above the absorption edge energy. The Fourier transformed EXAFS spectra recorded at the *K*-edges of Co and Ga in  $\text{LiA}_x\text{Mn}_{2-x}\text{O}_4$  compounds with  $x=0.5$  are compared in Fig. 1. The Fourier transformation produces a pseudo radial distribution function of the local atomic environment around the probed element. Beyond the first coordination shell of six oxygens, the Fourier-transformed spectrum recorded at the Co edge contains peaks corresponding to Mn and Co neighbours in 16d octahedral sites only. This indicates that Co ions share the octahedral sites with Mn and that the

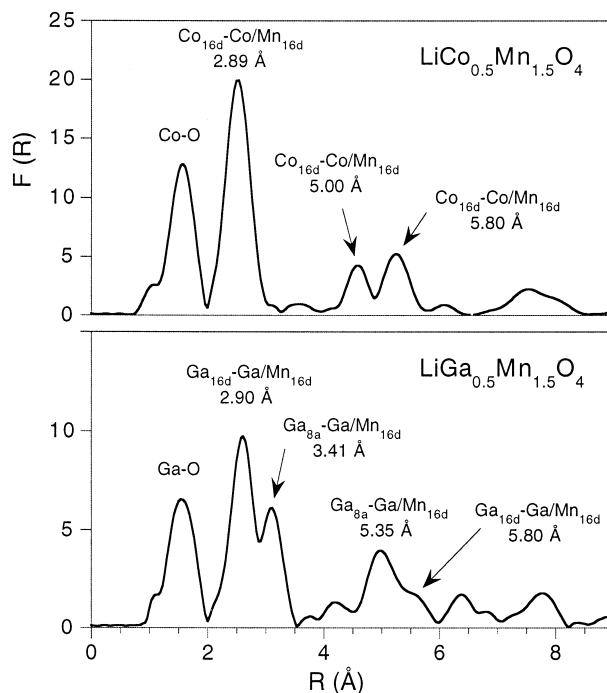


Fig. 1. Fourier-transformed EXAFS at the Co and Ga *K*-edges for  $\text{LiA}_{0.5}\text{Mn}_{1.5}\text{O}_4$  spinels. Dominant contributions to the Fourier peaks are indicated (the radial distributions are shifted ca. 0.3 Å low in the absence of a phase correction).

tetrahedral sites are occupied only by lithium ions, which produce negligible backscattering of the X-ray photoelectron. Curve-fitting refinements in wavevector space confirm that this is also the case for Cr and for Ti ions up to  $x=0.5$  in  $\text{LiA}_x\text{Mn}_{2-x}\text{O}_4$ . Co–O and Cr–O distances were determined to be 1.94 and 1.98 Å, respectively, which are the same as those in  $\text{LiCoO}_2$  and  $\text{LiCrO}_2$ . The Ti environment in Ti-substituted  $\text{LiMn}_2\text{O}_4$  is close to that determined by EXAFS for  $\text{Ti}^{4+}$  in the spinel  $\text{Li}_{4/3}\text{Ti}_{5/3}\text{O}_4$ , with an average Ti–O distance of 1.99 Å.

By contrast, the EXAFS spectrum at the Ga edge is a superposition of the octahedral site distribution and that of Ga in tetrahedral 8a sites. The Fourier transformation therefore shows interactions of Ga in both sites with neighbouring 8a and 16d Ga and neighbouring 16d Mn. Curve fitting of the EXAFS spectrum indicates that approximately 50% of the Ga is on tetrahedral 8a sites in the compound. It has been suggested that Ga substitution for Li in the tetrahedral 8a sites might improve cycling behaviour through stabilisation of the delithiated structure [1].

The effect of substitution on the Mn environment is observed at the Mn edge. Fig. 2 shows the Fourier transformed EXAFS spectra recorded at the Mn *K*-edge for various levels of trivalent ( $\text{Cr}^{3+}$ ) and tetravalent ( $\text{Ti}^{4+}$ ) substitution. The important trend in the spectra is an increase in the intensity of the EXAFS signal with increasing trivalent substitution. This is evidence of a continuous increase in local order around the Mn ions as the  $\text{Mn}^{3+}$

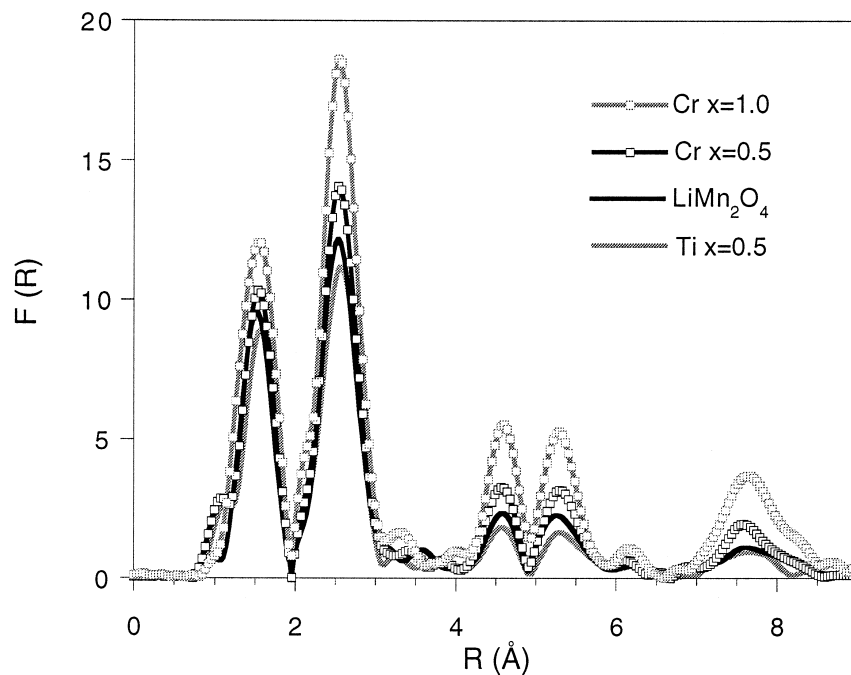


Fig. 2. Fourier-transformed EXAFS at the Mn *K*-edge for  $\text{LiA}_x\text{Mn}_{2-x}\text{O}_4$  spinels, showing the increase in local order with increasing trivalent substitution on the Mn site.

contribution is removed. The  $\text{Mn}^{3+}\text{O}_6$  octahedra appear to be distorted by Jahn–Teller stabilisation at a local level for all compositions where  $\text{Mn}^{3+}$  ions are present, even when they are relatively dilute in the lattice, and even though the compounds all produce XRD patterns for cubic spinels with no evidence for long-range ordering of the tetragonal distortion. The stabilisation of electrode capacity achieved by increasing the Mn oxidation state above 3.5 [3,4] is therefore likely to be due mainly to the suppression of long-range cooperative ordering of the Jahn–Teller  $\text{Mn}^{3+}\text{O}_6$  units when they are less concentrated in the structure.

Partial substitution of Mn can also reduce the overall magnitude of the long-range tetragonal lattice distortion when it occurs, for example during insertion of additional lithium into  $\text{LiMn}_2\text{O}_4$  to form  $\text{Li}_2\text{Mn}_2\text{O}_4$ . Our experiments with Cr substitution have shown that the *c/a* ratio in the tetragonal domains can be reduced from 16% in  $\text{Li}_2\text{Mn}_2\text{O}_4$  to < 4% in  $\text{Li}_2\text{CrMnO}_4$  [12]. EXAFS data recorded separately at the Cr and Mn *K*-edges for the tetragonal phases have shown that the local Cr environment remains cubic due to the regularity of the  $\text{Cr}^{3+}\text{O}_6$  octahedron, and it is the interspersions of these  $\text{Cr}^{3+}\text{O}_6$  units among the tetragonally-distorted  $\text{Mn}^{3+}\text{O}_6$  octahedra which disrupts and diminishes the cooperative elongation of the crystal along one axis.

### 3.2. Intrinsic disorder and Li migration

Additional lithium is often incorporated into  $\text{LiMn}_2\text{O}_4$  to stabilise the capacity of the material under extended

cycling, because only a small substitutional quantity is required to produce an increase in the average Mn oxidation state. However, it has been suggested that trivalent substitutions may cause less local disorder than lower-valence ions such as Li in the Mn sites of the spinel structure [1]. XAFS can provide only indirect information about the structure around Li ions, as it is not possible to probe this element directly using X-rays. A complementary approach to this problem is to use atomistic lattice simulation methods, which are well adapted to modeling polar inorganic solids such as lithium manganates at the atomic level [8]. The simulation techniques used here also have the advantage of calculating energies associated with lattice defects and migrating species, providing additional important information about the effects of substitution.

In Table 1, we give the interatomic distances for the fully relaxed local structures calculated around isolated substitutional ions in  $\text{LiMn}_2\text{O}_4$ , compared with EXAFS

Table 1  
Calculated interatomic distances (Å) around substitutional ions in  $\text{LiMn}_2\text{O}_4$  (EXAFS distances in parentheses), compared with average values for Mn

Element	M–O	M–Mn <sub>16d</sub>	M–Li <sub>8a</sub>
Ti <sup>4+</sup>	1.99 (1.99)	2.96 (2.96)	3.48
Cr <sup>3+</sup>	2.00 (1.99)	2.91 (2.91)	3.39
Co <sup>3+</sup>	1.96 (1.94)	2.88 (2.89)	3.38
Ga <sup>3+</sup>	2.00	2.91	3.39
Li <sup>+</sup>	2.11	2.81	3.30
Mn	1.96	2.91	3.41

Table 2

Li defect and migration energies (eV) around substitutional ions in  $\text{LiMn}_2\text{O}_4$ , compared with values for non-substituted  $\text{LiMn}_2\text{O}_4$

Element	Li 8a vacancy	Li 16c interstitial	Li Frenkel	Li vacancy jump
$\text{Ti}^{4+}$	8.53	−5.59	1.47	0.99
$\text{Cr}^{3+}$	9.21	−6.03	1.59	0.80
$\text{Co}^{3+}$	9.30	−6.06	1.62	0.69
$\text{Ga}^{3+}$	9.30	−6.03	1.64	0.73
$\text{Li}^+$	10.25	−7.22	1.52	0.69
$\text{LiMn}_2\text{O}_4$	9.06	−5.82	1.62	0.72

results where possible. The simulations, which have used the interatomic potentials derived for the binary oxides [9], reproduce closely those local structures determined by EXAFS, including distortions in the neighbouring octahedral site sublattice. We note that while the trivalent substitutions produce only small deviations from the bulk structure,  $\text{Ti}^{4+}$  and  $\text{Li}^+$  ions on Mn sites are predicted to produce relatively large changes in local structure.

Table 2 gives calculated energies for the formation of Li vacancies in 8a tetrahedral sites and Li interstitials in 16c octahedral sites neighbouring the substitutional ions in the simulated lattices. These two energies combine to give the energy for Li Frenkel disorder in the immediate environment of the substitutional ion. The trends in the calculated values clearly show the importance of the local charge distribution in determining the Li site energies. As the charge on the substitutional ion is lowered from  $\text{Ti}^{4+}$  to  $\text{Li}^+$ , the Li 8a vacancy energy increases, and the energy for formation of a Li interstitial species in a 16c site decreases. The relative energies for Li vacancies can be correlated with the different distortions in the 8a sublattice in the calculated local structures, in which 8a lithium ions are relaxed toward the lower valence substitutionals, and away from more highly charged  $\text{Ti}^{4+}$ . Also given in Table 2 are the activation energies calculated for Li migration between two 8a sites neighbouring the substitutional ion, using our previously described model for an 8a vacancy jump [8]. These results predict that highly charged and larger, more polarisable substitutional ions (such as  $\text{Ti}^{4+}$  and  $\text{Cr}^{3+}$ ) will raise the energy for lithium ions to migrate through 8a–16c–8a channels in the local environment. More extensive calculations using molecular dynamics methods are planned.

### 3.3. Formation of protonated defects

Protonic species commonly form in oxides to compensate charge defects, and are frequently present in manganese oxide electrode materials. In the case of lithium manganates, protons transferred to the surface of the material from the surrounding medium are known to diffuse into the bulk lattice by exchange with lithium ions, particularly in the case of  $\text{Li}(\text{Li}_x\text{Mn}_{2-x})\text{O}_4$  type spinels [13]. The

protonic species formed in the spinel can be very stable and difficult to remove without degrading the structure of the material [14], and will therefore reduce the lithium-insertion capacity and cyclability. Proton–lithium exchange may therefore represent a problem for long-term storage of lithium manganese electrodes in electrolytes containing acidic species.

It is important to understand the conditions for the formation of protonated defects in lithium manganates. Data from infrared and inelastic neutron scattering spectroscopies show that protons inserted into spinel manganese oxide bond to lattice oxygen ions to form mainly hydroxyl species [14]. The substitutional energies and orientations of hydroxyl groups in oxides may be modeled atomistically using an O–H interaction described by an attractive Morse potential [15]. Our calculations for hydroxyl species in spinel manganese oxide show an energy preference of 3.6 eV for hydroxide ions to form at oxygen sites coordinating both an octahedral 16d and tetrahedral 8a vacancy over oxygen sites coordinating a tetrahedral 8a vacancy only [8,16]. Furthermore, the fully-relaxed configuration calculated for the hydroxyl species in this model, illustrated in Fig. 3, predicts successfully the atomic arrangement recently determined by neutron diffraction [17]. The tetrahedral–octahedral vacancy pair is therefore the critical defect species for protonation of the lattice. Such vacancy pairs are present in lithium manganates prepared at temperatures  $< 600^\circ\text{C}$ , or may be formed during the extraction of lithium from ‘lithium-rich’ spinel phases  $\text{Li}(\text{Li}_x\text{Mn}_{2-x})\text{O}_4$  in which lithium ions occupy both tetrahedral and octahedral (Mn) sites. Substitution of Mn by species such as  $\text{Ga}^{3+}$  which partly position on tetrahedral 8a sites, displac-

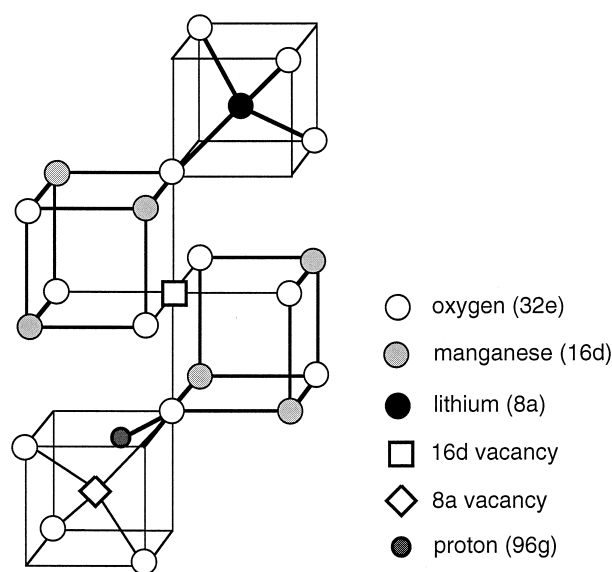


Fig. 3. Orientation of the hydroxyl group formed by protonation of an oxide ion coordinating the 8a–16d vacancy pair in spinel manganese oxide.

ing Li into octahedral 16d sites, will also be susceptible to form this defect.

### Acknowledgements

The authors thank the Royal Society (UK) for a European Science Exchange Programme joint project grant. B.A. is supported by a New Zealand Science and Technology Post-Doctoral Fellowship.

### References

- [1] G. Pistoia, A. Antonini, R. Rosati, C. Bellitto, G.M. Ingo, *Chem. Mater.* 9 (1997) 1443.
- [2] J.M. Tarascon, E. Wang, F.K. Shokoohi, W.R. McKinnon, S. Colson, *J. Electrochem. Soc.* 138 (1991) 2859.
- [3] R.J. Gummow, A. de Kock, M.M. Thackeray, *Solid State Ionics* 69 (1994) 59.
- [4] G.G. Amatucci, C.N. Schmutz, A. Blyr, C. Sigala, A.S. Gozdz, D. Larcher, J.M. Tarascon, *J. Power Sources* 69 (1997) 11.
- [5] B. Ammundsen, G.R. Burns, D. Jones, J. Rozière, *Chem. Mater.* 8 (1996) 2799.
- [6] J.D. Gale, *J. Chem. Soc., Faraday Trans.* 93 (1997) 629.
- [7] B.G. Dick, A.W. Overhauser, *Phys. Rev.* 112 (1958) 90.
- [8] B. Ammundsen, M.S. Islam, J. Rozière, *J. Phys. Chem. B.* 101 (1997) 8156.
- [9] G.V. Lewis, C.R.A. Catlow, *J. Phys. C: Solid State Phys.* 18 (1985) 1149.
- [10] N.F. Mott, M.J. Littleton, *Trans. Faraday Soc.* 34 (1938) 485.
- [11] B. Ammundsen, D.J. Jones, J. Rozière, *J. Solid State Chem.* 141 (1998) 294.
- [12] B. Ammundsen, D.J. Jones, J. Rozière, F. Villain, *J. Phys. Chem. B.* 102 (1998) 7939.
- [13] B. Ammundsen, P.B. Aitchison, G.R. Burns, D.J. Jones, J. Rozière, *Solid State Ionics* 97 (1997) 269.
- [14] B. Ammundsen, G.R. Burns, D.J. Jones, J. Rozière, *Chem. Mater.* 7 (1995) 2151.
- [15] M. Cherry, M.S. Islam, J.D. Gale, C.R.A. Catlow, *J. Phys. Chem.* 99 (1995) 14614.
- [16] B. Ammundsen, M.S. Islam, D.J. Jones, J. Rozière, *Mol. Cryst. Liq. Cryst.* 311 (1998) 109.
- [17] B. Ammundsen, H. Berg, D.J. Jones, J. Rozière, R. Tellgren, J.O. Thomas, *Chem. Mater.* 10 (1998) 1680.